OPTICAL DIFFRACTION OF THE Z LATTICE IN CANINE CARDIAC MUSCLE

MARGARET A. GOLDSTEIN, JOHN P. SCHROETER, and RONALD L. SASS

From the Department of Medicine, Section of Cardiovascular Sciences, and the Department of Cell Biology, Baylor College of Medicine, Fondren-Brown Cardiovascular Research and Training Center of The Methodist Hospital, Houston, Texas 77030, and Departments of Biology, Chemistry, and Physics, William Marsh Rice University, Houston, Texas 77001

ABSTRACT

Optical diffraction patterns from electron micrographs of both longitudinal and cross sections of normal and anomalous canine cardiac Z bands have been compared. The data indicate that anomalous cardiac Z bands resembling nemaline rods are structurally related to Z bands in showing a repeating lattice common to both. In thin sections transverse to the myofibril axis, both electron micrographs and optical diffraction patterns of the Z structure reveal a square lattice of 24 nm. This lattice is simple at the edge of each I band and centered in the interior of the Z band, where two distinct lattice forms have been observed. In longitudinal sections, oblique filaments visible in the electron micrographs correspond to a 38-nm axial periodicity in diffraction patterns of both Z band and Z rod. We conclude that the Z rods will be useful for further analysis and reconstruction of the Z lattice by optical diffraction techniques.

KEY WORDS muscle · diffraction · ultrastructure · Z band · myocardium

The ultrastructure of normal Z bands *in situ* in several vertebrate skeletal muscles has been reported (6, 14, 16, 23, 25, 26). The ultrastructure of nemaline or rod bodies of Z disc origin has also been studied and has been compared to that of normal Z bands (3, 29). MacDonald and Engel (19) have compared Z lattices of skeletal muscle after different fixation techniques and after low ionic strength extraction. More recently, Stromer et al. (30) have compared Z lattices after selective extraction. These (19, 30) and other (31, 32) studies have shown structural similarity between normal Z bands and rod bodies from a muscle specimen of congenital rod myopathy. Schollmeyer et al. (28) have shown two proteins immunologically common to both structures. Z discs of the frog's sartorius and rod bodies of human nemaline myopathy samples extracted at low ionic strength bind anti-α-actinin and anti-tropomyosin.

Detailed studies of the cardiac Z lattice have not been reported, although the similarity of the cardiac Z band in cross section to the skeletal muscle Z band has been noted (5). Viewing the Z band as a regular lattice suitable for analysis by optical diffraction techniques, we have studied the Z lattice and its relationship to the adjacent lattice of thin filaments at rest length. We have tested the assumption that anomalous Z bands in cardiac muscle (4), termed "Z rods" in this paper, which appear similar to rod bodies in skeletal muscle, are structurally related to Z bands in cardiac muscle. We conclude from comparisons in three planes of section that the Z rod is structurally related to the Z band, and can be

used for further analysis and reconstruction of the Z lattice by optical diffraction techniques. Brief preliminary reports of this research have been published (8-11).

MATERIALS AND METHODS

Preparation of Muscles

Normal Z bands were analyzed in left anterior and posterior papillary muscles from four normal dog hearts (a special breed, 75% Labrador and 25% hound, maintained by the Baylor Breeding Farm, Huntsville, Tex.). Normal Z bands in anterior papillary (control) muscles from two other dog hearts, made partially ischemic for 30 min by ligation of the left circumflex artery, were also examined. Z rods were observed in control muscle of one of these two hearts.

Dog hearts were perfused through the left main coronary artery with 2% glutaraldehyde in phosphate buffer. The heart was removed and the papillary muscles were exposed. Strips of superficial fibers from the left anterior papillary muscle were clamped to prevent shortening during fixation, and were excised and placed in 4% paraformaldehyde-5% glutaraldehyde in phosphate buffer for 1 h at room temperature. Superficial fibers of middle portions of the strips away from the clamps were cut into 1-mm cubes and placed in fresh fixative for an additional 2 h. The tissue samples were rinsed in buffer 2-16 h, postfixed in 1% osmium tetroxide in phosphate buffer, dehydrated rapidly in ethanol, oriented, and embedded in Epon in flat Silastic molds (Ladd Research Industries, Inc., Burlington, Vt.). Semithin sections were stained with methylene blue-Azure II and were examined for orientation and searched for the presence of anomalous Z structures with the light microscope.

Electron Microscopy

Thin sections were cut on a Porter-Blum MT-2 ultramicrotome (Dupont Instruments, Sorvall Operations, Newtown, Conn.) by a diamond knife. The long axis of the myofibers was parallel to the knife edge for longitudinal sections. Sections were stained by immersion in a saturated solution of uranyl acetate in 50% ethanol for 5 min, followed by flotation on lead citrate for 3 min. Longitudinal sections of the block containing a cell with the Z rods were examined first. Then the part of the block containing this cell was reoriented by 90° and glued with epoxy to a blank Epon block and sectioned again. Identification of some of the Z rods in cross sections was insured by examination of at least three consecutive sections, each 40-50 nm thick. Thin sections were examined in an RCA EMU 4, a Philips 200 or 201, or a JEM 100 B electron microscope. The microscope was calibrated with a Fullam carbon grating (Ernest F. Fullum, Inc., Schenectady, N. Y.) for each group of negatives. Measurements of Z band and I band width were made with dial calipers (0.05 mm) on EM prints photographically enlarged two to three times to a final magnification of 30,000.

Optical Diffraction Analysis

EM positives (× 18,000) on Kodak high-contrast lantern slide plates were used as diffraction subjects. The beam from the laser was directed through a collimating system to the relevant area of the photographic plate, and the resulting diffraction pattern was focused by a two-lens system and recorded directly on film. An adjustable aperture could reduce the beam size from 1.5 to 0.4 cm to correspond to the area of interest on the micrograph. The area selected for diffraction was the region which gave the clearest and brightest diffraction pattern for a particular orientation of the lattice, and was marked on a corresponding print of the electron micrograph. This area did not always correspond to the region of the micrograph which appeared to have the most clearly ordered image. Spurious diffraction effects due to emulsion irregularites were minimized by immersing the photographic plate between two optical flats in a fluid matching the refractive index of the emulsion. The system was calibrated by photographing the diffraction pattern of a square grid of known spacing each time a set of diffraction patterns was recorded.

Reciprocal values of lattice spacings were measured directly from the photographic recordings of the diffraction pattern. The variation in these measurements in the range of spacings recorded was from 0.15 to 0.30%. The precision with which a lattice spacing could be determined thus depended mainly on the degree of section compression and distortion during specimen preparation. Only micrographs containing both Z bands and several A band regions were used. The A band lattice was assumed to be truly hexagonal. The interfilament spacings of thick filaments were first measured in A bands in cross sections. The largest and most consistently observed spacing was 44.1 nm, and this value was taken as the minimally distorted A spacing. For each micrograph, the A spacings were calculated and the micrograph was dimensionally corrected to fit the above model. These corrections were then applied to the measured Z spacings from that same micrograph. In all cases, the correction implied either small random dimensional changes or compression in a single direction. This distortion was most noticeable in cross sections. In longitudinal sections, the A band spacings were generally in close agreement with a nearest thick filament spacing of 44.1 nm and a transverse repeat along the thick filaments of 42.9 nm.

RESULTS

General Features

In our initial studies of the Z lattice, emphasis was on the Z rods. Throughout our work on the

Z lattice in normal muscle, our results with the Z rods have remained in the foreground. Therefore, we have kept them in the foreground in the following presentation in the belief that the advantages of studying this structure more than compensate for the limited sample so far at hand. Detailed analysis of one papillary muscle from one of the six canine hearts was carried out to analyze both Z rods and normal Z bands in a single block and in a single cell in both longitudinal and cross sections. Semithin sections from 12 blocks of tissue processed from this control canine papillary muscle were examined with the light microscope. All of the cells, except for the one cell containing the Z rods, were uniform in appearance. Normal myofibrils in longitudinal sections of this block selected for further analysis with the electron microscope had a sarcomere length of 2.36 ± 0.005 μm (n = 60). In micrographs of longitudinal sections of the Z rods used for optical diffraction, the sarcomere length of adjacent myofibrils was 1.99 ± 0.01 μm (n = 25). Z rods varied in width from 0.12 to 0.37 μm (n = 45), and in length from 0.4 up to 1.5 μm (n = 35). They were sometimes continuous with adjacent Z bands, but were not always symmetrically placed with respect to these Z bands.

The optical transforms reported herein are interpreted on the basis of two-dimensional reciprocal lattices. Each such projected structure will be independently indexed using conventional Miller indices, hk. A single set of diffraction lines will be designated by (hk), and a form of symmetrically related lines will be designated $\{hk\}$. The h index will normally refer to the horizontal reciprocal axis (the equatorial direction from longitudinally oriented micrographs). Distances reported as $1/d_{hk}$ are directly obtained from measurements of the optical transform. The concept of a layer line refers to a linear array of reflections of constant value of k. A row line is a linear array of reflections of constant h. Optical transforms from three orientations of both Z rods and Z bands are used in this study.

Cross Sections of Z Rods

A cross section of Z rods from this muscle is seen in Fig. 1*a*. The rods vary in size and shape. Within a single rod, a shift in orientation of the lattice or a greater spacing between the lattice lines of a given direction with a corresponding decrease in density appears similar to the fault lines in mammalian skeletal muscle described by Rowe and Morton (27). The crosscut axial filaments observed in this lattice and shown schematically as uniform dots in the diagrams in Fig. 2 vary in size and shape, often appearing as diamond-shaped figures and triangles. Smaller connecting filaments are visible between the axial filaments, and form a pattern of small squares as diagrammed in the region marked "Interior" in Fig. 2*b*. Vesicles of the sarcoplasmic reticulum are seldom seen and do not encircle the Z rods as they do the Z band in cardiac muscle.

Optical diffraction patterns of 18 different areas of Z rods in cross sections were recorded. All patterns from cross sections of both Z rods and Z bands can be interpreted on the basis of a square lattice as illustrated in a diagram in Fig. 2. Diffraction patterns from the I band region adjacent to the Z region are typically those of a simple square lattice of ~ 24 × 24 nm. This simple lattice is hereafter referred to as the large square. A representation of a diffraction pattern from the I band is also shown at the bottom left in Fig. 2*c* i. This pattern consists of a square array of diffraction spots with a gradual decrease in intensity with increasing diffraction angle.

In the region of transition between I band filaments and axial Z filaments, the crosscut filaments form a square lattice of the same dimensions as that found in the I band. The first order axial reflections, {10}, from the diffraction pattern (d = 24 nm) decrease in intensity and at times disappear, corresponding to the observed transition from a simple to a centered lattice. Concomitantly, the reflections of the form {20} (d = 12 nm) grow in intensity (Fig. 2*c* ii and 2*c* iii), corresponding to the observed increasing presence of scattering matter parallel to the edges of the large lattice square, but spaced one-half of a cell length apart, subdividing the large square into four small squares.

A diffraction pattern from the interior portion of a Z rod shown in Fig. 1*b* is taken from the region circled in Fig. 1*a*. The corrected dimensions of 23.3 × 23.6 nm for the centered square lattice as measured from this pattern are consistent with the average observed square lattice of edge dimension 23.9 nm (σ = 0.6 nm, n = 18) obtained from patterns from all regions of the Z rod. A representation of this type of pattern is shown at the bottom right in Fig. 2*c*. The {10} reflections (d = 24 nm) are completely absent. The {20} reflections (d = 12 nm) are very intense compared to the {11} reflections (d = 17 nm).

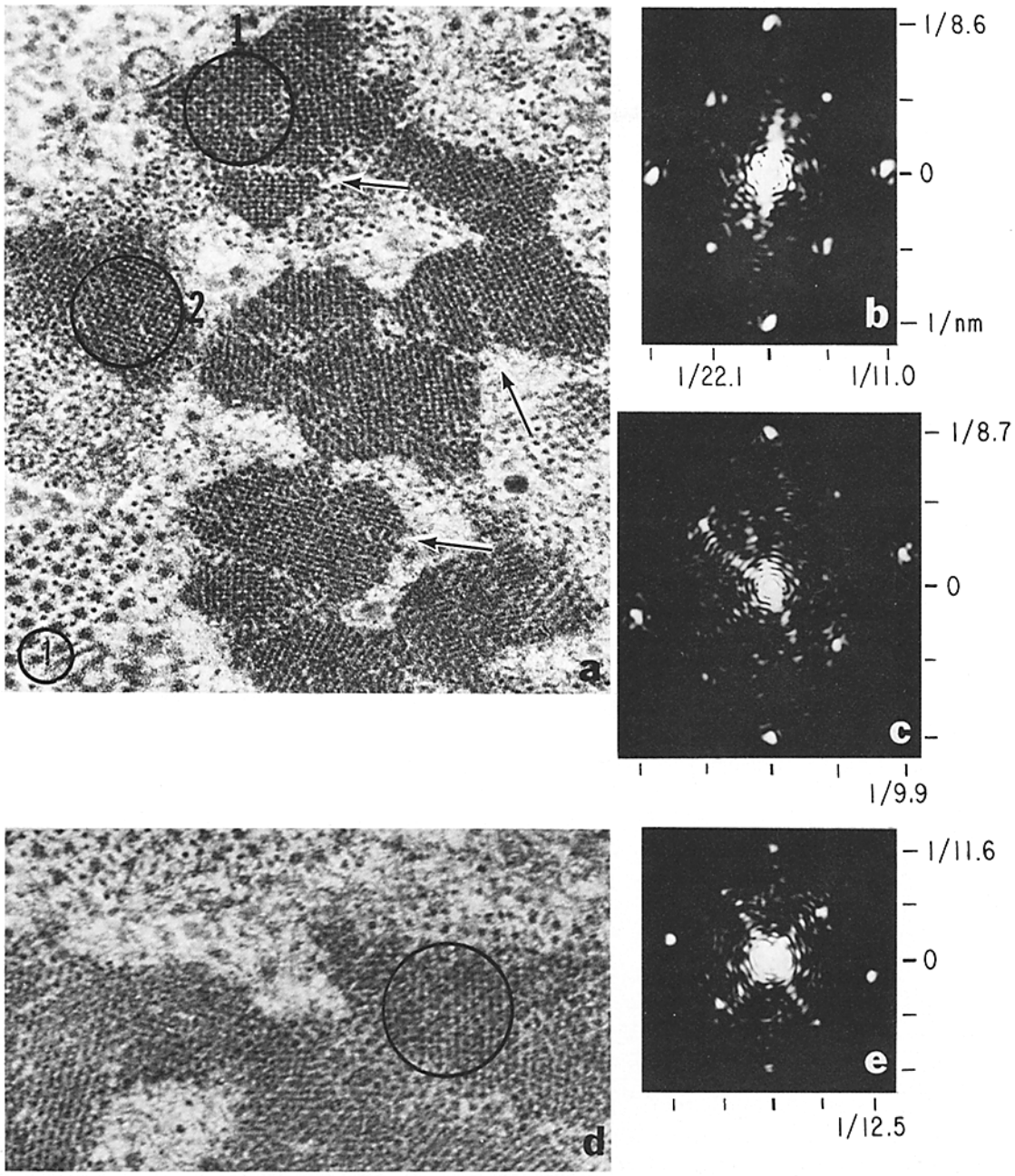

FIGURE 1 Two cross sections of Z rods from the same cardiac muscle cell used for longitudinal sections. The optical diffraction patterns are oriented in the same direction as the corresponding electron micrograph except for (*c*) which has been rotated by 25°. × 96,000. (*a*) This micrograph exhibits distortion of the square Z lattice to a rectangular lattice due to compression shown also in the A band lattice. The Z rods exhibit large and small lattice squares oriented in the same direction as the I squares. A local shift in orientation of lattice planes or a patch of greater lattice spacing in a Z rod is occasionally observed (arrows). These regions are somewhat suggestive of the basket weave pattern seen in the cardiac Z band. (*b*) An optical diffraction pattern of region 1 circled in (*a*). The observed (02) and (20) reflections are 1/8.6 and 1/11.0 nm^{-1}, and correct to second orders of (01) and (10) of values 1/23.3 and 1/23.6 nm^{-1}, respectively, when the distortion factor obtained from A band measurements is compensated as described in Materials and Methods. The pattern indicates a centered square lattice after correction. (*c*) An optical diffraction pattern of region 2 circled in (*a*). The observed (02) and (20) reflections are 1/8.7 and 1/9.9 nm^{-1}, but correct to 1/12.0 and 1/11.9 nm^{-1}, respectively. (*d*) The circled region of the rod at the upper right of the micrograph shows interruptions of the large and small square lattices seen in (*a*), and shows the appearance of filaments along the diagonals. The small square lattice is either absent or obscured even though some of the filaments are visible. (*e*) The optical diffraction pattern indicates a small square lattice 11.6 × 12.5 nm with diagonals at 16.1 and 18.4 nm. The reflections at 1/18.4 nm^{-1}, (11), and at 1/12.5 nm^{-1}, (20), are the more prominent pairs.

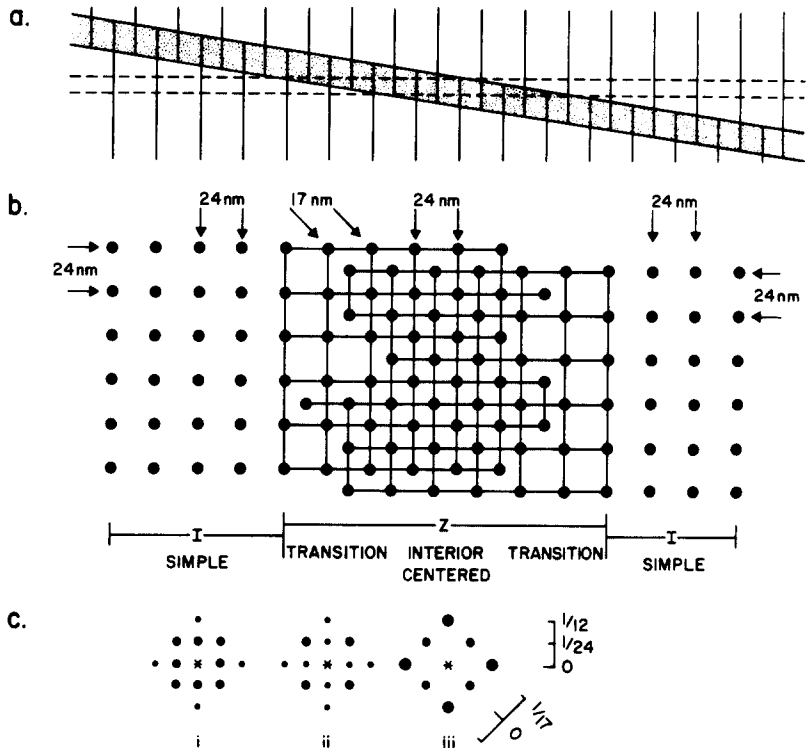

FIGURE 2 Diagram of successive sections through the Z band perpendicular to the fiber axis. (*a*) Longitudinal section of Z band between two I bands having interfilament distances of 24 nm. Cross section indicated by parallel dashed lines is perpendicular to the fiber axis, but not to the Z band. (*b*) Cross section of Z band which shows relationship of Z lattice to adjacent thin filaments and the transition zones from one end of Z band through middle of Z band to other end. The crosscut filaments of the Z band are called axial filaments. They are direct extensions of the adjacent thin filaments, and they interdigitate to form a centered square lattice. (*c*) Diagrammatic optical transforms of model lattices constructed as shown in the three regions of (*b*).

Fig. 1*c* is a diffraction pattern taken from region 2 in Fig. 1*a*. Note that this pattern of a centered lattice is somewhat skewed. Although the electron micrograph appears highly ordered, its diffraction pattern indicates that the orientation in region 2 is not as good as that in region 1. The resolution and symmetry of the diffraction pattern depends on both the regularity and orientation of the Z lattice, so that the region selected by eye from the electron micrograph does not necessarily give the best quantitative information.

The circled region in Fig. 1*d* is characterized by the lack of connecting filaments in some of the large squares and most of the small squares, and the presence of some filaments along the diagonals. There are also crosscut thin filaments in the region just above the circle. The optical diffraction pattern of this circled region, shown in Fig. 1*e*, is similar to the diffraction pattern in Fig. 1*b*. The {20} reflections (d = 12 nm) suggest a centered lattice, but the pair of intense reflections from the form {11} suggest scattering matter along the diagonal of the large square. Such diffraction features are consistent with the observed structure in the electron micrograph, and suggest a variable filamentous array for the Z rod in cross section.

Cross Sections of Z Bands

Electron micrographs of cross sections of cardiac Z bands are similar to those of Z rods (compare Fig. 1*a* with Fig. 3*a*). The optical diffraction patterns more precisely define these similarities. Both electron micrographs and optical diffraction patterns indicate a square lattice. As in the case of the Z rod, there is a transition from a simple lattice near the junction with the I band to a centered lattice in the interior of the Z band. The transition region in Fig. 3*a* is like that

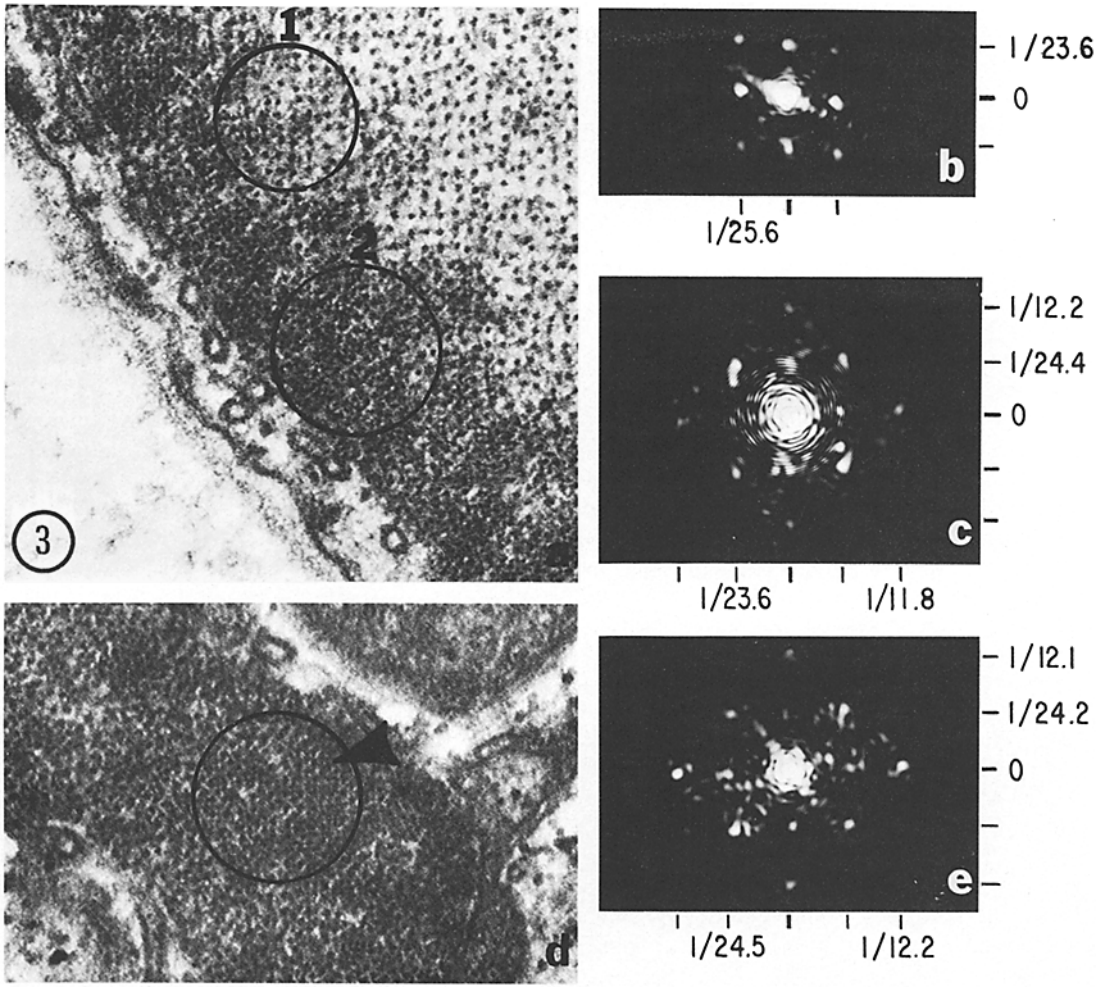

FIGURE 3 Electron micrographs and optical diffraction patterns of successive sections through the Z band perpendicular to the fiber axis. (*a*) A cross section of a normal canine heart cell showing crosscut axial filaments of the Z band having the same diameter as thin filaments immediately subjacent to the Z band. × 80,000. (*b*) The optical diffraction pattern of an I band region (1 in Fig. 3*a*) subjacent to the Z band has (01) and (10) reflections at 1/23.6 and 1/25.6 nm^{-1}. (*c*) The optical diffraction pattern of region 2 circled in (*a*) has (01) and (10) reflections at 1/24.4 and 1/23.6 nm^{-1}, which correct to 1/23.7 and 1/23.7 nm^{-1}, and two sets of reflections {11} at 1/17.0 nm^{-1}, one stronger, and (02) and (20) reflections at 1/12.2 and 1/11.8 nm^{-1}. The 1/17.0 nm^{-1} reflections are along an axis at 45° to primary axis of pattern. (*d*) Another cell in the same section as that in (*a*). The Z band exhibits both the large and small square lattice pattern shown best at arrowhead, and some patches of basket weave pattern seen best when the micrograph is rotated 45°. × 80,000. (*e*) The optical diffraction pattern of region circled in (*d*) shows (01) and (10) reflections at 1/24.2 and 1/24.5 nm^{-1}, (02) and (20) reflections at 1/12.1 and 1/12.2 nm^{-1}, and two sets of reflections, {11} at 1/17.0 nm^{-1}, again, one set stronger.

diagrammed in Fig. 2. The diffraction pattern in Fig. 3*b* (I band circled in Fig. 3*a*) reveals a simple lattice 23.6 × 25.6 nm (see diagram in Fig. 2*c*). The adjacent transition region in Fig. 3*a* exhibits the same orientation and spacing of the large square lattice. In the diffraction pattern (Fig. 3*c*) the intensity of the {10} reflections is diminished, and the intensities of the {20} spots and the {11} reflections are enhanced. Fig. 3*e* shows the diffraction pattern of the Z band in another cell of this same specimen of normal cardiac muscle shown in Fig. 3*d*. This diffraction

pattern is that of a region which is partially centered (lattice dimensions 24.2 × 24.5 nm) and is very similar to the pattern of the Z rod shown in Fig. 1*b*.

Cardiac Z bands from two other canine hearts prepared in the same way predominantly exhibited the "basket weave" pattern (Figs. 4, 5) previously described by others in cross sections of skeletal muscle (19, 23). The optical diffraction patterns shown in Fig. 4*b*, *c*, taken from two adjacent regions (shown in Fig. 4*a*), exhibit additional higher order spots not seen in the Z rods. This may be due to increased ordering in comparison with similar areas of diffracted Z rod images. However, it may also be due to higher order symmetry features peculiar to the image of the basket weave lattice. The strongest spots are the {11} reflections in all four diffraction patterns shown from this muscle (Fig. 4*b*, *c*, *e*, and *g*), exactly as expected from the obvious alignment of Z filaments with diagonals of the centered lattice in the basket weave pattern. Note the increasing intensities of the {10} reflections in the transforms from Fig. 4*b* to *g*, and the corresponding increase in the prominence of the axial crosscut filaments in the micrographs Fig. 4*a–f*. The large square lattice in Fig. 4*a* is a centered lattice with respect to the crosscut filaments, but the diffraction pattern in Fig. 4*b* does not show the prominent {20} reflections characteristic of a centered lattice. This type of pattern results because the symmetry of the four filaments along the diagonals arranged about each axial filament is different for the two sets of crosscut filaments (see Fig. 10*f*). The {10} reflections shown in Fig. 4*c*, *e*, and *g* are more intense than those of Fig. 4*b*. This ordering can be verified by inspection of region 2 in Fig. 4*a*; one of the large square arrays dominates this area of basket weave. Note that in this region the weave appears "loosened." The dimensions of the large square in region 2 of Fig. 4*a* (24.3 nm) are also slightly larger than those in region 1 (22.6 nm). The diffraction pattern in Fig. 4*b* resembles the pattern shown diagrammatically in Fig. 10*f*, and the pattern in Fig. 4*c* is suggestive of a transition region. Fig. 4*d* does exhibit a transition region and the {10} reflections in the corresponding diffraction pattern in Fig. 4*e* are more intense than they are in Fig. 4*c*. Another transition region shown in Figure 4*f* contains even fewer diagonal filaments, and the corresponding diffraction pattern in Fig. 4*g* exhibits nearly equal intensities of the {10} and {11} reflections. Higher order reflections are much weaker in this pattern. The average Z band lattice edge spacing measured in diffraction patterns obtained from 18 Z bands in five micrographs of three different hearts is 23.9 nm (σ = 0.8 nm).

Fig. 5 shows in a single section transverse to the myofibril axis of a canine cardiac cell, all three regions diagrammed in Fig. 2. Both the small square lattice and the basket weave lattice are clearly visible in the interior of the Z band shown at the top third of the micrograph. The transition region, which includes some I band as well as Z band in the section thickness, is in the

FIGURE 4 Electron micrographs and optical diffraction patterns of successive sections through the Z band perpendicular to the fiber axis. × 90,000. (*a*) An electron micrograph from a control canine heart sample. The basket weave is the predominant pattern visible, except in the two dense regions shown at the arrowheads. In the first region selected for optical diffraction, the lattice is more dense and more closely spaced than in the second. (*b*) Optical diffraction pattern from region 1 in (*a*). Reflections at 1/22.3, (01), 1/11.2, (02), 1/22.9, (10), 1/11.5, (20), and 1/16.0 mm^{-1}, {11}, are visible, as well as higher order spots. (*c*) Optical diffraction pattern from region 2 in (*a*). Reflections at 1/23.7, (01), 1/24.9, (10), and 1/17.0 nm^{-1}, {11}, are present. In both (*b*) and (*c*), the {11} reflections for the diagonal 17.0-nm spacing are most prominent. (*d*) Electron micrograph of Z band in another cell in this sample showing transition from the end of the I band into the Z band. A dominant large square lattice is overlain with hints of the diagonal basket weave. (*e*) Optical diffraction pattern from circled region in (*d*) has reflections at 1/23.1, (01), 1/25.0, (10), and 1/16.7 nm^{-1}, {11}, and corresponds well with the visible large square lattice having scattering material along the diagonals. (*f*) Another cross section of normal cardiac Z band taken from the block also shown in longitudinal section (Fig. 8*a*) exhibits the basket weave pattern mixed with small square pattern. The uncentered large square pattern shows some scattering material along the diagonals. (*g*) The optical diffraction pattern has (01) and (10) reflections at 1/24.4 and 1/22.1 nm^{-1}, and (02) and (20) reflections at 1/12.2 and 1/11.0 nm^{-1} and {11} reflections at 1/17.4 and 1/16.1 nm^{-1}.

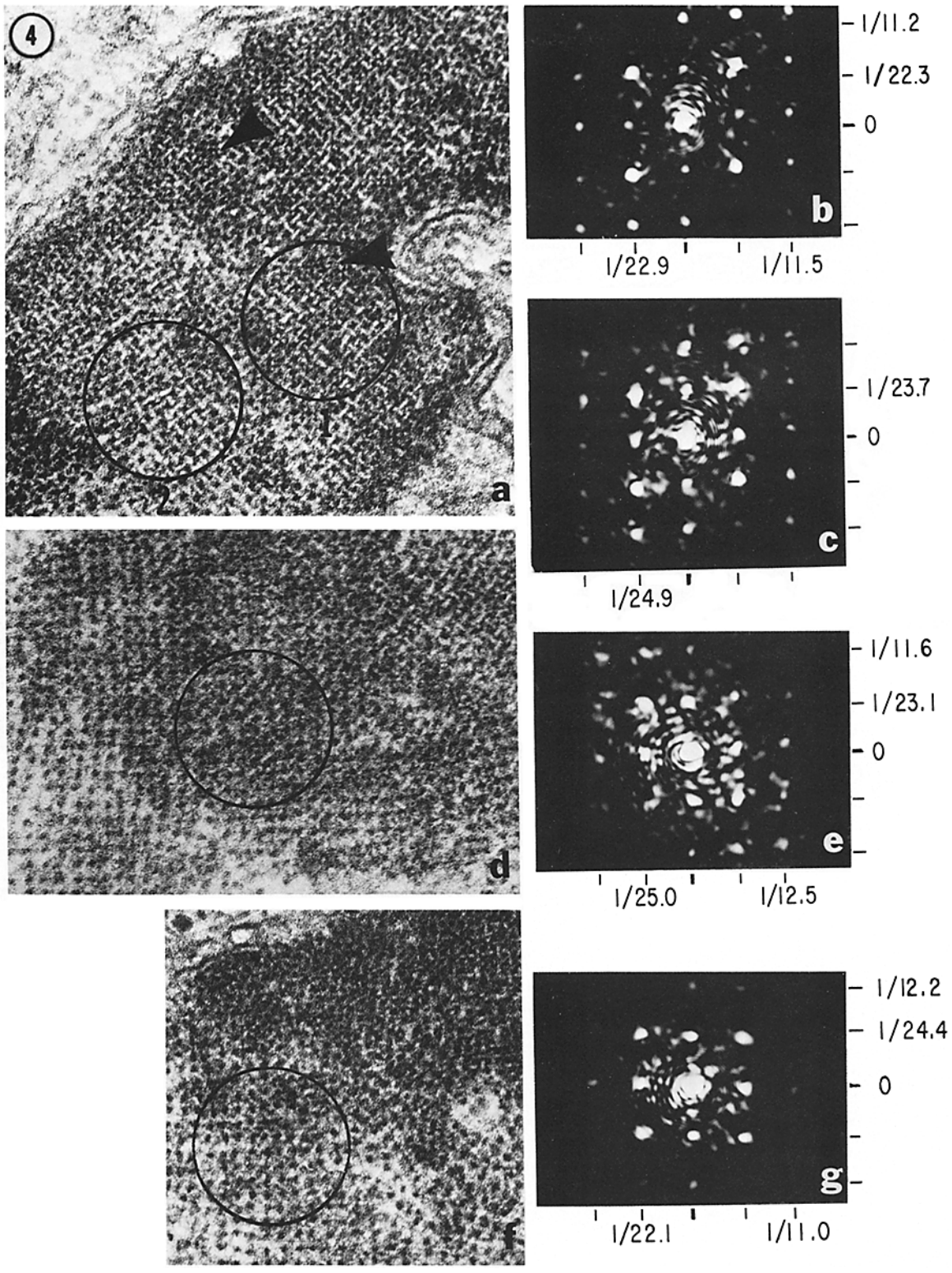
4
a
b
1/11.2
1/22.3
0
1/22.9
1/11.5
c
1/23.7
0
1/24.9
d
e
1/11.6
1/23.1
0
1/25.0
1/12.5
f
g
1/12.2
1/24.4
0
1/22.1
1/11.0

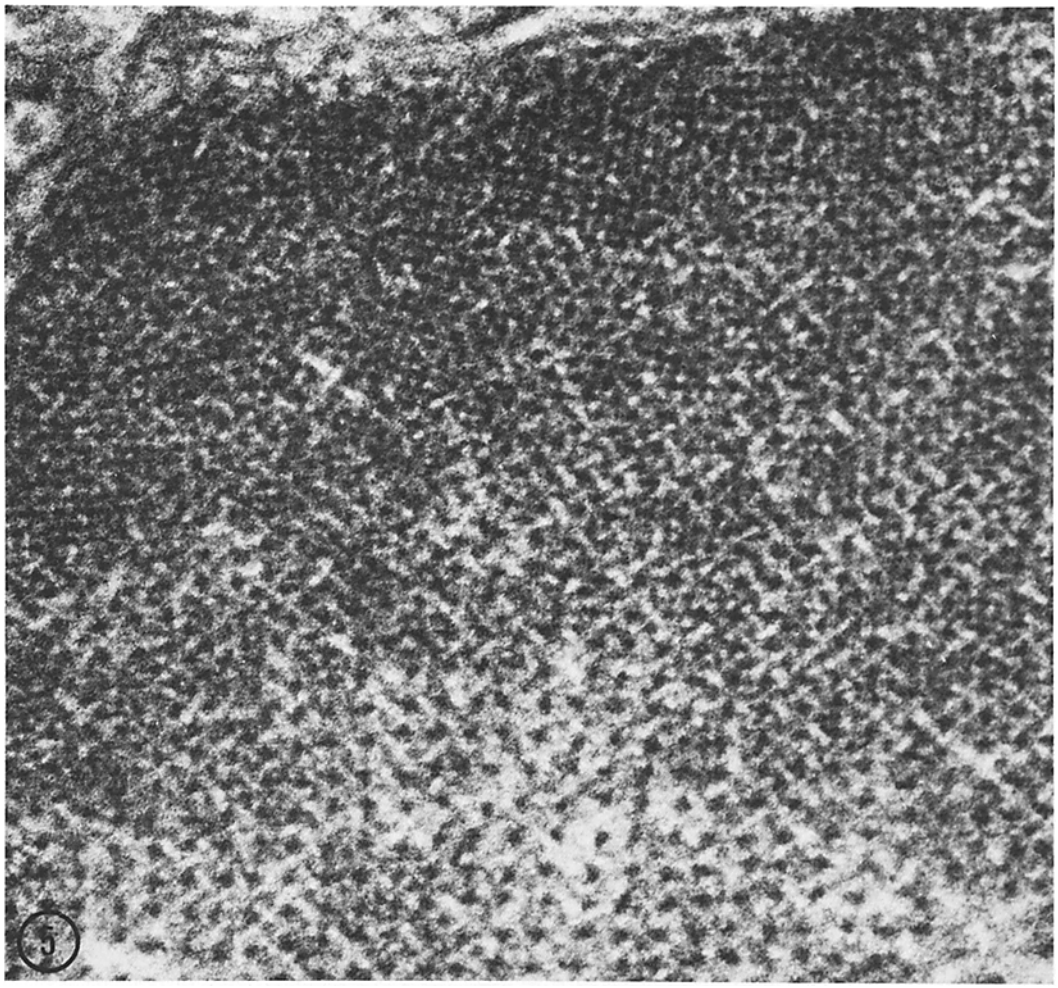

FIGURE 5 An electron micrograph of a cross section of normal canine cardiac muscle at the level of the Z band. Note adjacent regions exhibiting the basket weave and the small square pattern. × 182,000.

middle third of this micrograph. The subjacent I band is at the bottom. The Z band exhibits both lattice patterns previously observed by others in skeletal muscle.

Longitudinal Sections of Z Rods

From the cross sections of Z rods and Z bands, two longitudinal planes are predicted for maximal positive reinforcement of axial filament arrays. One such plane is indicated by the double arrows in Fig. 2*b* at 24 nm apart. A longitudinal section of Z rod (representative of such an orientation) is shown in Fig. 6*a*. Axial filaments of similar thickness and density are spaced 11.5 nm laterally, and alternate axial filaments appear to be continuous with one I set, the remainder with the other set. Variations appear along the filaments, tending to mark an axial period associated with near transverse and oblique lattice planes which can be seen by sighting along various directions of the Z rod image. Because each axial filament profile is produced by superimposition of 2–4 filaments within the section thickness, these more or less periodic variations in density, thickness, and apparent continuity are not attributable to misalignment between single filaments and the plane of section, but are likely to represent features actually present and enhanced by superposition. The oblique planes at 20–25° off the longitudinal axis are associated with oblique projections or filaments lying between the axial filaments and giving them a periodially barbed appearance.

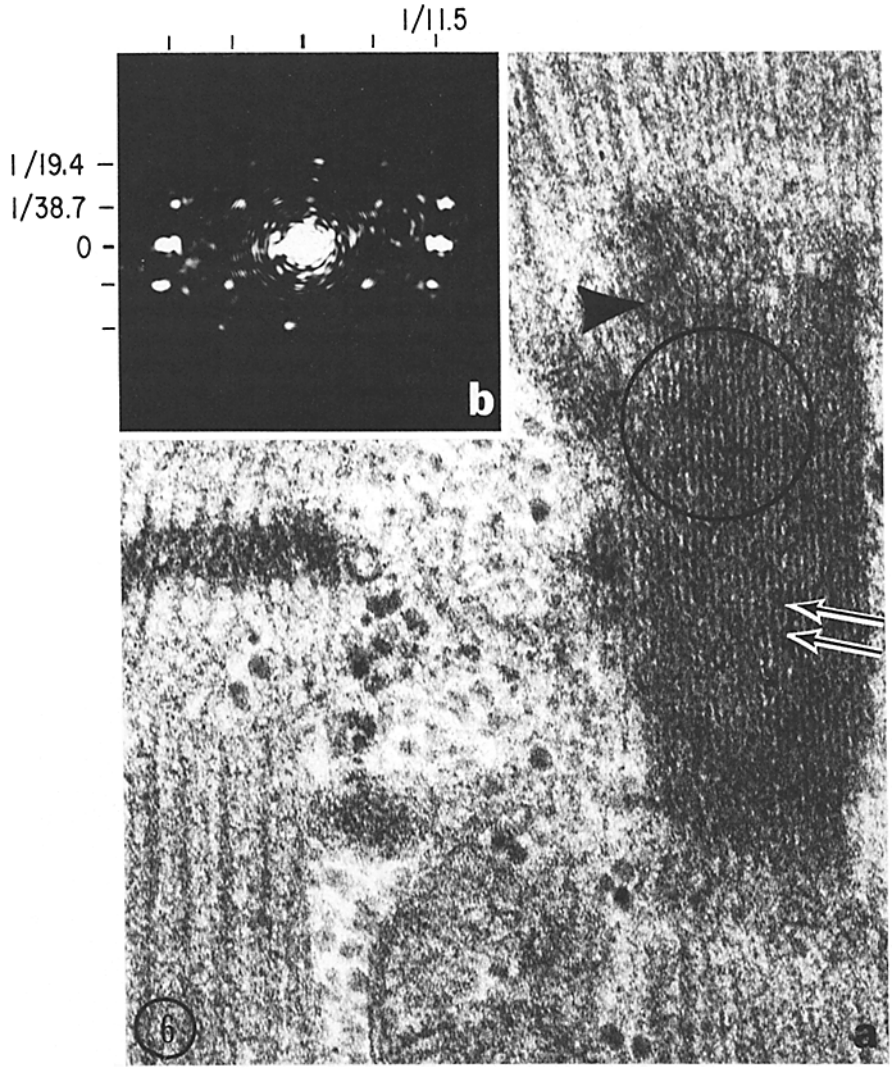

FIGURE 6 Electron micrographs and optical diffraction patterns of the Z rod in a longitudinal section in one of the two orientations predicted from cross sections. (*a*) A Z rod from a sample of canine papillary muscle previously shown in cross section. Axial filaments parallel to the fiber axis are spaced at 11.5 nm apart and have a transverse repeat every 38.7 nm (arrows). In some regions, the axial filaments vary in apparent thickness from 3 to 10 nm. A normal Z band is shown at the left. × 96,000. (*b*) Optical diffraction pattern from region shown in (*a*). An intense (20) equatorial reflection is at 1/11.5 nm^{-1}. Off-meridional reflections above and below both the first and second order equatorial reflections form layer lines at 1/38.7 and 1/19.4 nm^{-1}. The second order layer line is represented only near the meridian. The (21) reflection at 1/10.6 nm^{-1} is more intense than the ($2\bar{1}$) reflection at 1/11.8 nm^{-1}. The lattice axis defined by the array of reflections is not perpendicular, but shows a reciprocal lattice axial angle of 81°.

Fig. 6*b* from the circled region in Fig. 6*a* is representative of the optical diffraction patterns observed for this orientation of Z rods. The most intense reflection is the second order equatorial spot (20) at 1/11.5 nm^{-1} which corresponds to the center-to-center spacing of axial filaments as seen in this projection. The first order equatorial reflection (10) is occasionally observed with very weak intensity, and indicates small differences in the image densities of alternate axial filament profiles.

First and second layer lines (k = 1, 2) in Fig.

6*b* which measure 1/38.7 and 2/38.7 nm^{-1}, respectively, suggest a periodic structure transverse to the axial filaments (see double arrows in Fig. 6*a*). The first layer line contains off-meridional spots above and below the second order equatorial reflections corresponding to $1/d_{21}$ = 1/10.6 nm^{-1}, and $1/d_{2\bar{1}}$ = 1/11.8 nm^{-1}. One pair corresponding to the closer distance in real space is often more intense than the other pair. The angle of 81° between the (21), (20), and (2$\bar{1}$) triad of reflections and the equator suggests that the axial repeating unit of one filament in the Z rod is displaced with respect to that of the adjacent filament by ~ 4 nm. In diffraction patterns of Z rods of this same orientation in other sections of this cell (n = 17) skewed row lines were observed (81° ± 3°), but in a few patterns (n = 4) row lines perpendicular to the equator were found.

The second orientation of the Z rod in longitudinal section which gives reinforcement by superimposition of axial filaments is shown in Fig. 7*a*. The interfilament spacing here is 17 nm and corresponds to one-half the diagonal distance predicted from a 24 nm square arrangement of crosscut filaments previously viewed in cross section in Figs. 1 and 2. Two optical diffraction patterns characteristic of this orientation are shown in Fig. 7*b* and *c* from adjacent regions circled in Fig. 7*a*. Both show (10) equatorial spacings of 17.1 nm; Fig. 7*b* shows one pair of first layer line off-meridional spots at $1/d_{11}$ = 1/15.2 nm^{-1}, and Fig. 7*c* shows two pairs of off-meridional spots at $1/d_{11}$ = 1/15.6 nm^{-1}. A weak pair of fourth order near meridional reflections (04) gives a measured value of $1/d_{04}$ = 4/38.0 nm^{-1}. It is notable that the row lines here are perpendicular to the equator, not at 81° as in Fig. 6*b*. The average value for the transverse periodic structure was 38.5 nm ± 0.5 (σ = 2.1). There was no correlation between presence or absence of skew and variation in intensity of the off-meridional spots.

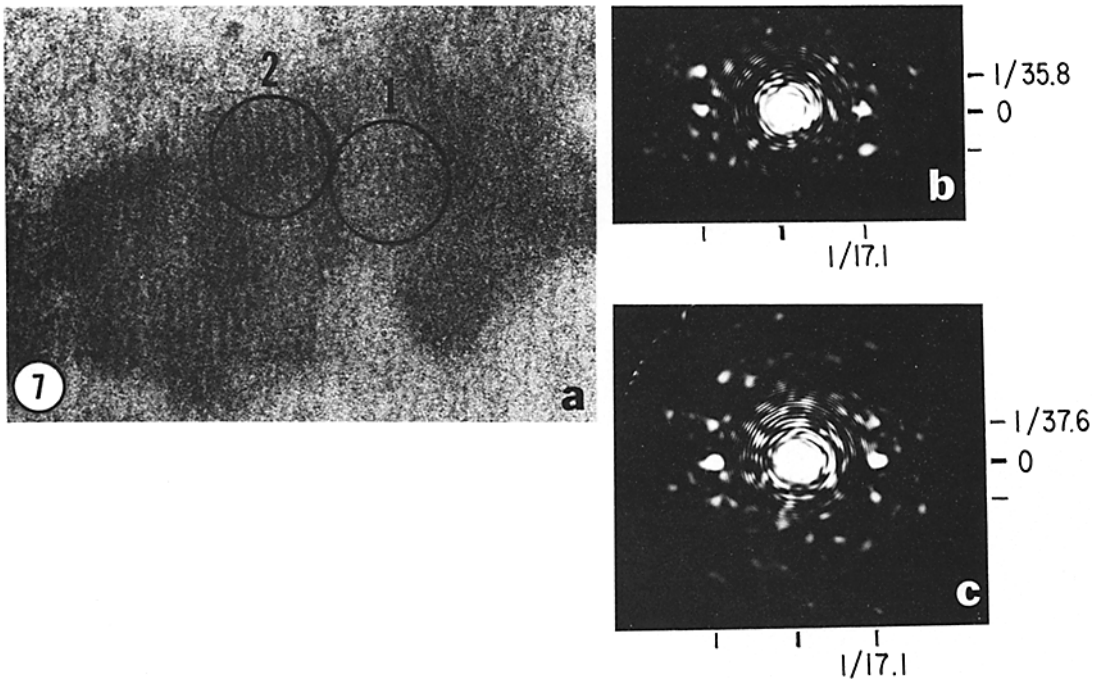

FIGURE 7 Electron micrograph and optical diffraction patterns in another longitudinal section. (*a*) A Z rod that is oriented in longitudinal section to show interfilament spacings of one-half the diagonal of the 24-nm square array previously shown for the Z rod and Z band in cross section. × 96,000. (*b*) Optical diffraction pattern from region 1 marked in (*a*). The (10) equatorial reflection is at 1/17.1 nm^{-1} and the layer line at 1/35.8 nm^{-1}. (*c*) Optical diffraction pattern from region 2 marked in (*a*). The (10) equatorial reflection is also 1/17.1 nm^{-1}; the 1/37.6 nm^{-1} layer line spots are directly above and below the major equatorial reflections.

Longitudinal Sections of Z Bands

Longitudinal sections of cardiac Z bands next to Z rods, of adjacent cells, and of cells from other canine hearts prepared in the same manner, were used for measurement of sarcomere length (2.16 ± 0.02 μm, σ = 0.10) and Z band width (109 nm ± 2, σ = 13) (n = 360). From these sections, 19 Z bands were analyzed by optical diffraction. Fig. 8*a* is an electron micrograph of a longitudinal section from a block that was subsequently reoriented to give the cross section shown in Fig. 4*f*. The average sarcomere length in this cell and in other cells in this block was 2.35 μm ± 0.005 μm (n = 50). The optical diffraction patterns shown in Fig. 8*b*, *d* from regions marked in Fig. 8*a*, *c*, resemble the patterns from the Z rod shown in Fig. 6*b*. The equatorial spacings of 25.7 and 12.9 nm in Fig. 8*b*, and 28.0 and 14.3 nm in Fig. 8*d* suggest a square array of larger dimensions (26.0-28.0 nm) than the 24.0-nm lattice observed in the Z rod. One set of off-meridional reflections is slightly more intense than the other set in both these patterns. The first order equatorial reflections, {10} observed in Fig. 8*b*, *d*, were seldom observed in the Z rod. These spacings correspond to the more prominent large square array observed in the basket weave Z pattern previously shown in a cross section of this specimen.

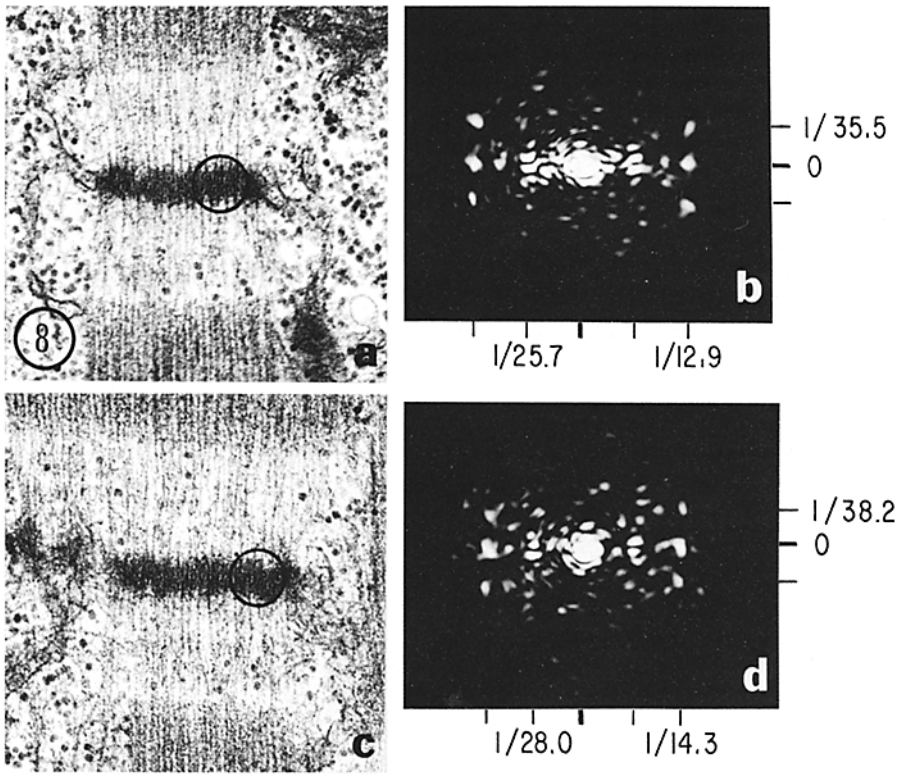

FIGURE 8 Electron micrograph and optical diffraction patterns of normal Z bands in longitudinal section. (*a*) Longitudinal section of papillary muscle from a normal dog previously shown in cross section (Fig. 4*f*). × 40,000. (*b*) In the optical diffraction pattern from region circled in Fig. 8*a*, a strong (10) first order equatorial reflection, as well as the second order (20) reflection, are shown at 1/25.7 and 1/12.9 nm^{-1}, and correspond to values obtained from the cross sections of Z bands in this specimen. Layer lines at 1/35.5 nm^{-1} with strong second row line reflections are present as previously shown in the Z rod, and again one pair is more intense. (*c*) Longitudinal section of papillary muscle from a normal dog previously shown in cross section (Fig. 4*f*). × 40,000). (*d*) An optical diffraction pattern taken from region circled in Fig. 8*c* has a visible (10) equatorial reflection at 1/28.0 nm^{-1}, and a more intense (20) reflection at 1/14.3 nm^{-1}.

A longitudinal section of another muscle block from this same heart is shown in Fig. 9*a*. Four Z bands in two sarcomeres exhibit the same two orientations previously shown in longitudinal sections of the Z rod. The optical diffraction patterns in Fig. 9*b* correspond to regions marked in the electron micrograph (Fig. 9*a*). The patterns for regions 1 and 2 are similar to the ones shown in Figs. 6 and 8, and correspond to the first of the two longitudinal orientations. The optical diffraction pattern for region 1 contains a major second order equatorial reflection ($1/d_{20}$ = 1/12.7 nm^{-1}), and a weaker first order reflection ($1/d_{10}$ = 1/24.6 nm^{-1}). Off-meridional reflections above and below the second order equatorial reflections differ in intensity, but are equally spaced ($1/d_{21}$ = 1/12.2 nm^{-1}). The values for the first order equatorial reflections {10} are within the range encountered for the large square array as measured in cross sections and longitudinal sections of both Z rod and Z band. The Z bands in another filament bundle of similar sarcomere length are shown at the left in Fig. 9*a*. Diffraction patterns from regions 3 and 4 are shown at the left in Fig. 9*b*. This orientation is such that axial filaments are prominent and appear continuous with the thin filaments, and is similar to the second one shown (Fig. 7*a*) for longitudinal sections of the Z rod. The major equatorial reflections are $1/d_{10}$ = 1/18.3, and $1/d_{10}$ = 1/17.4 nm^{-1}, and correspond to half the diagonal distance of a 24-nm square. The (21) and (2$\bar{1}$) spots are also observed as in the Z rod and one set is consistently more intense. In Fig. 9 B 3, the (2$\bar{1}$) pair of reflections is replaced by a pair of reflections of somewhat smaller d value. In Fig. 9 B 4, the (21) and (21) reflections are both absent and are replaced by two pairs of reflections indicative of the (21) and (2$\bar{1}$) pairs of Fig. 9 B 1. These observations suggest that scattering material associated with those reflections may curve and cross in a plane different from the axial filaments.

In summary, we have observed that both Z rods and Z bands in cardiac muscle are arranged in a square lattice centered in the interior and simple near the Z-I junction. The average edge dimension of this square is 23.9 nm (σ = 0.5) for the Z rod and 23.9 nm (σ = 0.8) for the Z band as observed from optical diffraction measurements on cross-sectional electron micrographs. Longitudinal sections yield the slightly higher values of 24.2 nm (σ = 0.6) and 24.7 nm (σ = 1.2) for the edge of the Z rod and Z band square lattice, respectively. In all cases, the first order equatorial spacing corresponds to the separation distances between adjacent I filaments in each neighboring

FIGURE 9 *A* Electron micrograph of cardiac Z bands showing the two orientations previously shown for the Z rod. This longitudinal section is from another block of the same normal cardiac muscle shown in Figs. 4*f* and 8. Z bands at each of two different sarcomeres, one at the right and one at the left, were analyzed. The orientation of the lattice in the two Z bands at the right is like the one previously shown in Figs. 2*a*, 6, and 8. The orientation of the lattice in the Z bands of the sarcomere at the left is similar to that shown in Fig. 7. × 26,000. *B* Optical diffraction patterns from the four regions in A. For region 1, the major equatorial reflection is (20) at 1/12.7 nm^{-1}, but the first order (10) is visible at 1/24.6 nm^{-1}. Off-meridional reflections, on the 1/37.6 nm^{-1} layer line, above and below the second order equatorial reflections, are present in most patterns of the longitudinal sections, but sometimes, only the predominent pair is visible. For region 2, the (10) equatorial reflection at 1/27.2 nm^{-1} and the more intense (20) at 1/13.6 nm^{-1} are present together with the off-meridional reflections above and below marking a layer line at 1/32.7 nm^{-1} in this case. The optical diffraction pattern from region 3 is typical for Z bands oriented to give spacings between axial filaments equal to the half-diagonal distance of the 24-nm square. The observed value for this pair of (10) equatorial reflections is 1/18.3 nm^{-1}. Again, off-meridional reflections are present as they were in Fig. 8*b* and *d*. The optical diffraction pattern from region 4 exhibits a 1/17.4 nm^{-1} equatorial reflection, but the off-meridional reflections now are different from those seen in Fig. 9*B* 3. Features producing the equatorial spot and features producing the layer line spots appear not to be coordinated with one another here as they were in Fig. 8*d*. The layer line spots occur on a row line about one-third farther from the origin than the equatorial. Neither the layer lines nor the row lines established by these spots are parallel to the orthogonal axis established by the equatorial line through the origin. Correspondingly, the actual appearance of region 4 is rather different from that of region 3, as if they were somewhat different views.

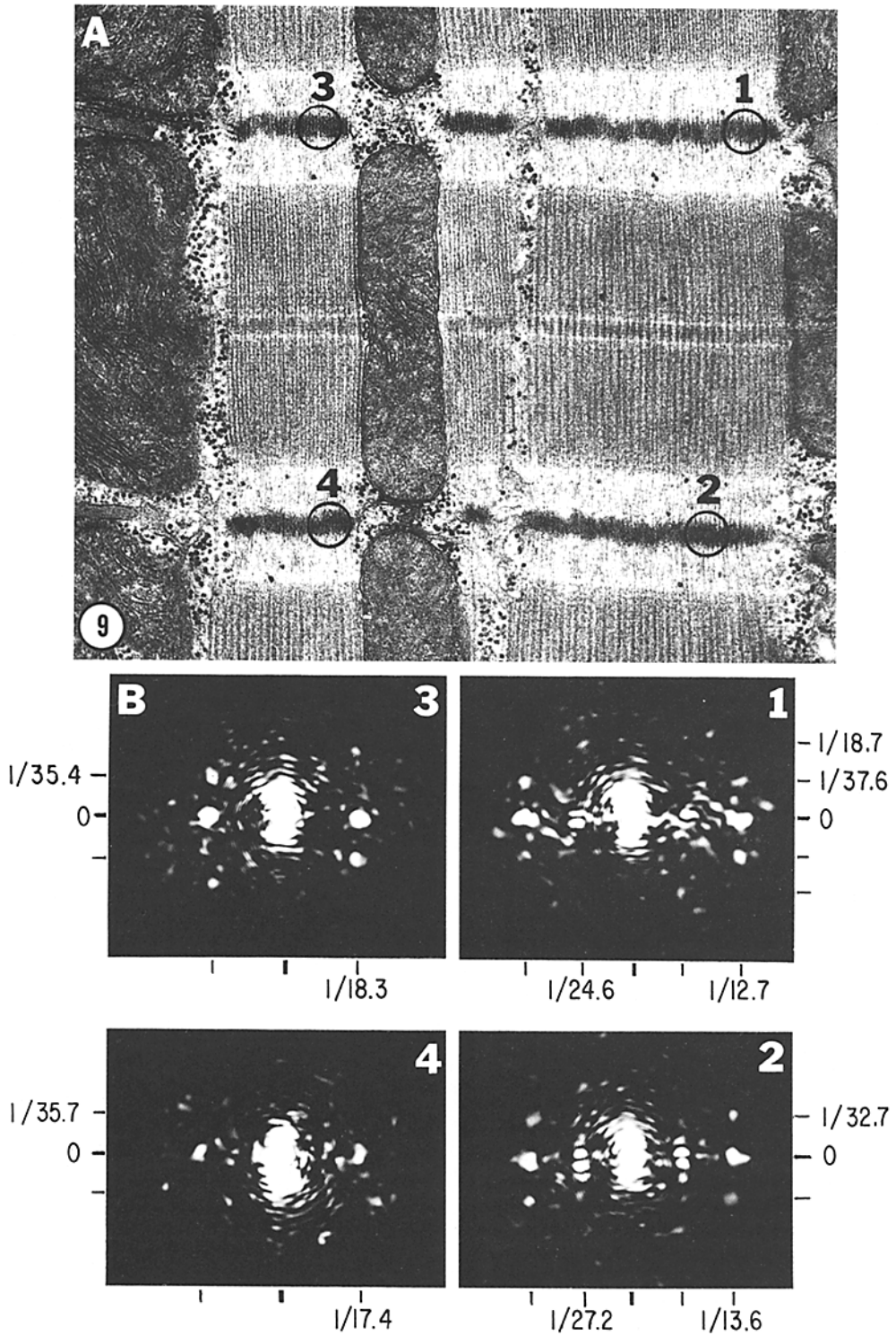
A
3
1
4
2
9
B
3
1
1/35.4
0
1/18.7
1/37.6
0
1/18.3
1/24.6
1/12.7
4
2
1/35.7
0
1/32.7
0
1/17.4
1/27.2
1/13.6

I band as measured by optical diffraction. The longitudinal sections also show the presence of an axial periodicity of 38.5 nm (σ = 2.1) and 38.0 nm (σ = 2.6) for the Z rod and Z band, respectively. Optical diffraction patterns from longitudinal sections of both Z rods and Z bands, both oriented along the large square lattice edge and at 45° to this edge, show strong characteristic diffraction from oblique lattice planes. These reflections are observed on the first layer line above and below the principal equatorial reflections, and correlate with oblique filaments or barbs on the axial filaments observed in the electron micrographs.

DISCUSSION

Optical diffraction analysis of Z rods and Z bands in cardiac muscle reveals similarities in lattice dimensions in both cross sections and longitudinal sections. Z bands of normal width in the same cell with the Z rods and in adjacent normal cells in the same block of anterior papillary muscle generated diffraction images like Z bands from another anterior papillary muscle and from anterior and posterior papillary muscles from normal dogs.

Some variability in lattice dimensions was observed, but the range of corrected values taken from Z bands in different hearts was no greater than the range from Z bands within a single cell. The constant volume behavior of sarcomeres was not a source of significant Z lattice variation in this study because the sarcomere length was near or at rest length (range = 1.98–2.38 μm) throughout this material. Because shrinkage of muscle protein lattices occurs during dehydration and embedding processes (2, 20, 24), values for both the A band lattice and the Z band lattice are probably low. The observed variability in the Z lattice spacings after correction suggests that the Z lattice is more flexible than the A lattice, or more susceptible to differing shrinkage from cell to cell and from preparation to preparation. Larger lattice spacings were observed both in cross sections and in longitudinal sections where less dense material of the Z lattice was visible. Differing amounts of extracted Z amorphous dense material might also make the Z lattice more susceptible to distortion.

Optical transforms of the Z lattice in cross section can be compared to transforms of two model lattices drawn from proposed Z models in the literature (7, 15–17, 25). Two of these filamentous lattices have been recently discussed by Franzini-Armstrong (6). Type A shown in Fig. 10*c* consists of an array of lines to form large and small squares with a centered square array of dots, and can arise from several models (6, 15; particularly Fig. 8 for reference 6). The optical diffraction pattern of the type A model lattice is a sum of two optical diffraction patterns; lines only as in Fig. 10*b* and dots only as in Fig. 10*a*. The type B lattice has scattering material at 45° angles to the I squares (6, Fig. 6). The optical diffraction pattern of the type B lattice (lines only, Fig. 10*d*, and dots only, Fig. 10*a*) differs from type A in the relative intensities of the {11} reflections as compared to the {10} reflections.

The line drawing in Fig. 10*f* is our idealized version of the region of the Z lattice in cross section as seen in Fig. 4*a*, and resembles published versions of the basket weave appearance of skeletal muscle (23). The diffraction pattern in Fig. 10*f* is generated from a transparency of Fig. 10*e* and resembles the actual pattern shown in Fig. 4*b*. By combining patterns such as those in Fig. 10*e* and 2*c* i with the pattern in 10*f*, it is possible to obtain diffraction patterns similar to those seen in Fig. 4*c*, *e*, and *g*. Optical transforms of the cardiac Z lattice in cross section contain features suggested by previous models and can be interpreted as a complex lattice which contains two distinct lattice forms. The extent to which these two forms superimpose or interconvert is not yet known.

The optical diffraction patterns of cross sections of Z bands are not exactly like the patterns observed for the Z rod, but are closely related. The appearance of transition and composite patterns suggests that two different scattering patterns either interconvert or coexist in the Z band. One pattern of small squares parallel to the I squares may be attributed to ordered arrays of dense matrix material. A second pattern (Fig. 10*e*) may be related to the oblique filaments seen in longitudinal sections. Some of the patterns may appear different because of variable extraction of the ordered arrays of dense matrix material. The fact that a pattern like the fully centered one shown in Fig. 1*b* was not seen in the Z band, is consistent with the hypothesis that the Z band was always partially extracted. Electron micrographs show a more uniform and a more dense lattice in the Z rods. Previous studies have shown that the Z rod in skeletal muscle is resistant to extraction (30). However, low ionic strength extraction of the Z rod can transform the appearance

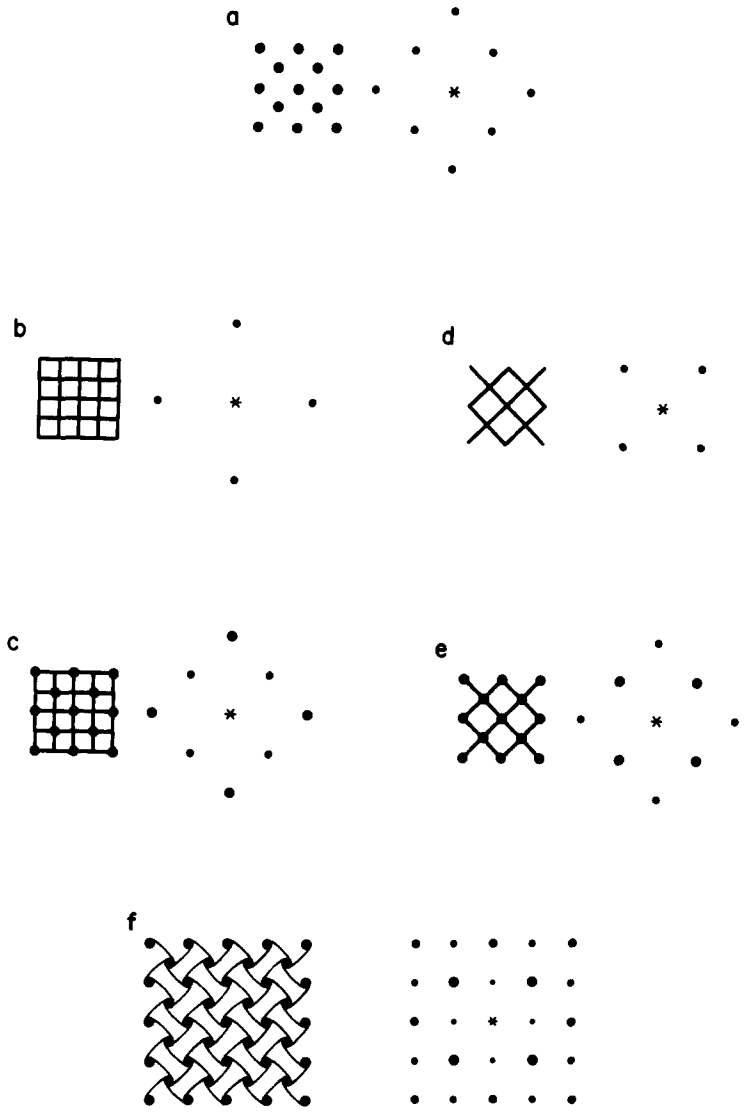

FIGURE 10 Models of Z band components in cross section and corresponding optical transforms.

to that of the basket weave pattern in cross sections, as shown by MacDonald and Engel (19), and to a prominent array of oblique filaments in longitudinal sections (30). Although this pattern may be a rearrangement of the matrix lattice, it is also possible that the extraction procedure has uncovered the second lattice type. This interpretation is consistent with the statement by Kelly and Cahill (15) that the matrix lattice occurs in serial sections next to the basket weave lattice. It is probable that the dense matrix lattice is easily disrupted in normal Z bands. The small square lattice in the Z band, when visible, is usually less discrete and fuzzier than in the Z rod.

If a given centered region contains both the basket weave and a superimposed matrix lattice, then the diffraction pattern is that of a composite of the two lattices, and different diffraction patterns arise depending on the relative amounts of the two lattice forms. Thus, if no matrix, all matrix, or a uniform amount of matrix is extracted throughout the Z band, then all structural units will be alike and will correspond exactly to the average unit indicated by the optical diffraction pattern. But, if partial extraction occurs in patchy fashion, the average structural unit will still be

the unit indicated by optical diffraction, by definition, but the actual structural units in different patches will be more or less unlike the average unit. Domains of the small square matrix lattice in the Z band are seen in the present study (Fig. 5) and have been observed by others in skeletal muscle (15, 17). The basket weave patterns shown in Figs. 4 and 5 give very regular optical transforms rich in higher order diffraction spots not obtained from the small square pattern of the Z rod or the Z band. When patches of the basket weave pattern occur in the centered lattice as in Fig. 3*a*, the 1/17 nm^{-1} spots can gain intensity as shown in Fig. 3*c*. The layer line values of 1/38 to 1/39 nm^{-1} in optical diffraction patterns of longitudinal sections of both Z rod and Z band suggest a lattice structure common to both. First and second order as well as zero order row lines are observed. The near meridional (01) reflection on the first layer line suggests an axial periodicity similar in value to periodicities reported by Stromer et al. (30) in nemaline rods before and after low ionic strength extraction. Stromer and co-workers have also described oblique filaments in the Z rod after low ionic strength extraction that are associated with a major repeat at 39.0 nm and a minor repeat at 19.5 nm. The presence of the second order near meridional (02) reflection in optical diffraction patterns of the cardiac Z rod suggests a repeat of every 19.5 nm in our preparations of fixed unextracted Z rods. A transverse repeat of 20 nm in electron micrographs of the Z rod in cat, dog, and human heart muscle has been reported (1, 4, 18).

Because the transverse periodicity of 38–39 nm in our study coincides in value and direction with that of troponin periodicity along thin filaments in the I band (12, 21, 22), the periodicity being measured in the case of the Z bands may be in the I band. Optical diffraction patterns from adjacent I bands exhibited the first order equatorial reflection seen in the diffraction pattern of the Z band. Such I patterns did not show a meridional reflection at 38.5 nm, even in the most clearly ordered electron micrographs, and did not show first and second order row lines characteristic of the Z lattice. This does not exclude the possibility that I filaments continue into the Z band, and that the near meridional reflection observed in the cardiac Z lattice may be partly due to an actin-tropomyosin periodicity in the axial Z filaments.

The more intense (21) and ($2\bar{1}$) reflections are characteristic of diffraction patterns of both Z rod and Z band, and strongly indicate that these structures share a common lattice. One pair of these spots is more intense both in Z rods and in Z bands. Two oblique sets of crossed filaments with one set thicker or formed from a double strand would be consistent with this pattern, but not consistent with the symmetry generally expected in such lattices. Another explanation involves section thickness. The 81° skewing of the row lines sometimes observed, suggests that the repeating unit of one axial Z filament may be displaced with respect to those of adjacent filaments by ~ 4 nm. In view of the orthogonal symmetry in transverse sections, it seems possible that the same displacement occurs along the viewing direction normal to the section plane of Fig. 4*a*. The projected effect of this feature on the image could complicate the apparent lattice structure of Z rods in longitudinal sections 50–75 nm thick. The Z band is susceptible to changes from extraction of matrix material and to distortion forces from both I bands which may affect the relative intensities of these spots and the skew of the row lines.

The most obvious differences between the Z band and the Z rod, in optical diffraction patterns of longitudinal sections, are the presence of the first order equatorial reflection in the Z band, and the suppression of the first order equatorial spot and the intensification of the second order spot in the Z rod. One explanation for this concerns the ratio of Z band interior (with its 12-nm side spacing) to Z band edge or I-Z region (with its 24-nm spacing) in the regions being analyzed. In the case of the Z rod, it is possible to position the laser beam so that only interior subunits and therefore only centered regions with 12-nm side spacings are analyzed. In the case of the cardiac Z band, axial extent is limited to three of four subunits, and two of these, i.e. those immediately next to the I band, are partially uncentered, so that the 24-nm side spacing becomes prominent. When the edge of the Z rod is analyzed (as in the region marked by the arrowhead in Figure 6*a*), a 23.7-nm equatorial spot is present, as well as the 11.5-nm equatorial reflection.

The Z band in cardiac muscle may project as a simple tetragonal lattice, but it becomes more complicated in the third dimension. Electron micrographs reveal a complex filamentous lattice with axial and oblique filaments, and varying

amounts of amorphous material. Oblique filaments are visible in electron micrographs of both Z rods and Z bands. The differing intensities of off-equatorial and off-meridional spots in diffraction patterns of longitudinal sections are consistent with the observation of oblique filaments in the electron micrographs, but there are problems with orientation of the lattice and superposition profiles. We do not know from these data if oblique filaments are continuous with or connected to the axial filaments which are recognizable in both cross sections and longitudinal sections, as the periodic association is not yet evidence for connection. More information about the oblique filaments, particularly data from other longitudinal and oblique planes, will be necessary before complete structural models of Z rods and Z bands can be established.

Our data extend previous observations from skeletal muscle to cardiac muscle. Our innovations include not only optical diffraction analysis of single specimens of Z structures, but also three plane analyses of single specimens of Z structures. The similarity of the lattice structures and of densities associated with the lattice in both the Z rod and the Z band observed by others in skeletal muscle (19, 30) are further revealed in our cardiac material. The optical diffraction data extend the evidence for a chemical similarity as a common lattice strongly implies common subunit structure. The Z rod is not pure tropomyosin, but exhibits the difference in structure between Z units and pure tropomyosin crystals first pointed out by Caspar et al. (2). It is true that some electron micrographs of Z rods (4) and Z bands (13) present features reminiscent of tropomyosin aggregates. Our studies of both Z rod and Z band reveal periodicities similar to tropomyosin, but a complex lattice arrangement which is fundamentally different. The measured lattice spacings of 38, 24, and 17 nm, suggest that binding sites, characteristic of many crystalline or regular aggregates containing tropomyosin (2), have formed a different arrangement of similar protein components in the Z rod and Z band.

By optical diffraction, we have defined the Z lattice in three planes. We have made models of the projection patterns of the lattice, formed by filaments visible in electron micrographs of cross sections, to show the several similar, but distinct, diffraction patterns that may be produced. We have alluded to the role of section thickness in presenting limited samples of extended or complex arrays as a factor responsible for some features of our diffraction patterns. When studied in this manner, the Z rod is similar to the Z band in cardiac muscle, but is more uniform and easier to orient spatially than most areas of the Z band. We conclude the Z rods will be useful for further analysis and reconstruction of the Z lattice by optical diffraction techniques.

We thank Mr. David L. Murphy for his excellent technical assistance, Doctors Joe G. Wood, Lea Rudee, and Charles W. Philpott for use of their electron microscopes and laboratory facilities, and Dr. Paul Donoho for use of the argon laser. We gratefully acknowledge Mr. Robert M. Lewis who surgically prepared the canine hearts. We thank Dr. Arnold Schwartz and Dr. Charles W. Philpott for helpful discussions. We especially thank Dr. Michael Reedy for a critical review of the manuscript.

This study was supported by U. S. Public Health Service grant HL 17376, in part by the Section of Myocardial Biology of the National Heart and Blood Vessel Research and Demonstration Center, Baylor College of Medicine, a grant-supported research project of the National Heart, Lung and Blood Institute, National Institutes of Health (NIH) HL 17269-02, by grant HL 05925, Contract NIH 71-2493, and by the American Heart Association, Texas Affiliate, Houston Chapter. Dr. Goldstein is the recipient of an NIH Research and Career Development Award–1K04 HL00321-01.

Received for publication 22 March 1977, and in revised form 25 July 1977.

REFERENCES

1. Bishop, S. F., and C. R. Cole. 1969. Ultrastructural changes in canine myocardium with right ventricular hypertrophy and congestive heart failure. *Lab. Invest.* **20**:219–229.
2. Caspar, D. L. D., C. Cohen, and W. Longley. 1969. Tropomyosin: crystal structure, polymorphism and molecular interactions. *J. Mol. Biol.* **41**:87–107.
3. Engel, A. G., and M. R. Gomez. 1967. Nemaline (Z-disc) myopathy, observations on the origin, structure and solubility of the nemaline structures. *J. Neuropathol. Exp. Neurol.* **26**:601–619.
4. Fawcett, D. W. 1968. The sporadic occurrence in cardiac muscle of anomalous Z bands exhibiting a periodic structure suggestive of tropomyosin. *J. Cell Biol.* **36**:266–270.
5. Fawcett, D. W., and N. S. McNutt. 1969. The ultrastructure of the cat myocardium. I. Ventricular papillary muscle. *J. Cell Biol.* **42**:1–45.
6. Franzini-Armstrong, C. 1973. The structure of a simple Z line. *J. Cell Biol.* **58**:630–642.

7. FRANZINI-ARMSTRONG, C., and K. R. PORTER. 1964. The Z disc of skeletal muscle fibrils. *Z. Zellforsch. Mikrosk. Anat.* **61**:661-672.
8. GOLDSTEIN, M. A., J. P. SCHROETER, and R. L. SASS. 1974. Optical diffraction analysis of the cardiac Z band. *Fed. Proc.* **33**:(II)1333.
9. GOLDSTEIN, M. A., J. P. SCHROETER, and R. L. SASS. 1974. Unit cell of Z lattice in cardiac and skeletal muscle. *J. Cell Biol.* **63**:114 a. (Abstr.).
10. GOLDSTEIN, M. A., J. P. SCHROETER, and R. L. SASS. 1975. Optical diffraction of the Z lattice in striated muscle. Proc. 33rd Annual Meeting, Electron Microscopy Society of America. Claitor's Publishing Division, Baton Rouge, La.
11. GOLDSTEIN, M. A., J. P. SCHROETER, and R. L. SASS. 1975. Z lattice in mammalian skeletal muscles having different Z band widths at rest length. *J. Cell Biol.* **67**:137 a. (Abstr.).
12. HANSON, J., V. LEDNEV, E. J. O'BRIEN, and P. M. BENNETT. 1972. Structure of the actin containing filaments in vertebrate skeletal muscle. *Cold Spring Harbor Symp. Quant. Biol.* **37**:311-318.
13. HUXLEY, H. E. 1963. Electron microscope studies of the structure of natural and synthetic protein filaments from striated muscle. *J. Mol. Biol.* **7**:281-308.
14. KELLY, D. E. 1967. Models of muscle Z band fine structure based on a looping filament configuration. *J. Cell Biol.* **34**:827-840.
15. KELLY, D. E., and M. A. CAHILL. 1972. Filamentous and matrix components of skeletal muscle Z discs. *Anat. Rec.* **172**:623-642.
16. KNAPPEIS, G. G., and F. CARLSEN. 1962. The ultrastructure of the Z disc in skeletal muscle. *J. Cell Biol.* **13**:323-335.
17. LANDON, D. N. 1970. The influence of fixation upon the fine structure of the Z disc of rat striated muscle. *J. Cell Sci.* **6**:257-276.
18. LEGATO, M. J. 1970. Sarcomerogenesis in human myocardium. *J. Mol. Cell. Cardiol.* **1**:425-437.
19. MACDONALD, R. D., and A. G. ENGEL. 1971. Observations on organization of Z disk components and on rod-bodies of Z disk origin. *J. Cell Biol.* **48**:431-436.
20. MILLMAN, B. M., and P. M. BENNETT. 1976. Structure of the cross-striated adductor muscle of the scallop. *J. Mol. Biol.* **103**:439-467.
21. O'BRIEN, E. J., P. M. BENNETT, and J. HANSON. 1971. Optical diffraction studies of myofibrillar structure. *Phil. Trans. Roy. Soc. London, Ser. B.* **261**:201-208.
22. OHTSUKI, I., and T. WAKABAYASHI. 1973. Optical diffraction studies on the structure of troponin-tropomyosin-actin paracrystals. *J. Biochem. (Tokyo).* **72**:369-377.
23. REEDY, M. K. 1964. The structure of actin filaments and the origin of the axial periodicity in the I substance of vertebrate striated muscle. (Discussion on article by J. Hanson and J. Lowy). *Proc. Roy. Soc., London Ser. B.* **160**:458-460.
24. REEDY, M. K., and A. E. BARKES. 1974. Disordering of myofibril structure due to fixation, dehydration, and embedding. *J. Cell Biol.* **63**:282 a. (Abstr.).
25. ROWE, R. W. D. 1971. Ultrastructure of the Z line of skeletal muscle fibers. *J. Cell Biol.* **51**:674-685.
26. ROWE, R. W. D. 1973. The ultrastructure of Z disks from white, intermediate, and red fibers of mammalian striated muscle. *J. Cell Biol.* **57**:261-277.
27. ROWE, R. W. D., and D. J. MORTON. 1971. Faults in the square lattice of mammalian skeletal muscle Z disks. *J. Cell Sci.* **9**:139-145.
28. SCHOLLMEYER, J. V., D. E. GOLL, M. H. STROMER, W. DAYTON, I. SINGH, and R. ROBSON. 1975. Studies on the composition of the Z disk. *J. Cell Biol.* **63**:303 a. (Abstr.).
29. SHY, G. M., W. K. ENGEL, J. E. SOMERS, and T. WANKO. 1963. Nemaline myopathy. A new congenital myopathy. *Brain.* **86**:793-810.
30. STROMER, M. H., L. B. TABATABAI, R. M. ROBSON, D. E. GOLL, and M. G. ZEECE. 1976. Nemaline myopathy, an integrated study: selective extraction. *Exp. Neurol.* **50**:402-421.
31. SUGITA, H., T. MASAKI, S. EBASHI, and C. M. PEARSON. 1973. Protein composition of rods in nemaline myopathy. *In* Basic Research in Myology. Proc. IInd International Congress on Muscle Diseases, Perth, B. A. Kakulas, editor. American Elsevier Publishing Co., Inc., New York, 298-302.
32. SUGITA, H., T. MASAKI, S. EBASHI, and C. M. PEARSON. 1974. Staining of the nemaline rod by fluorescent antibody against ^{10}s-actinin. *Proc. Jpn. Acad.* **50**:237-240.